Available online at www.sciencedirect.com
SCIENCE DIRECT®
Catalysis Today 98 (2004) 181–191
CATALYSIS TODAY
www.elsevier.com/locate/cattod

# Selective hydroconversion of a model mixture and hydrotreated FCC gasoline for octane enhancement

H. González[a,b,*], J. Ramírez[a,c], A. Gutiérrez-Alejandre[a], P. Castillo[a], T. Cortez[c], R. Zárate[c]

[a]*UNICAT, Dpto. de Ingeniería Química, Facultad de Química, U.N.A.M., Cd. Universitaria, 04510 México D.F., México*
[b]*Facultad de Ingeniería Química, Universidad Michoacana de San Nicolás de Hidalgo, Edificio M, Cd. Universitaria, 58060 Morelia, Michoacán, México*
[c]*Instituto Mexicano del Petróleo, Eje Central Lázaro Cárdenas #152, 07730 México D.F., México*

Available online 13 September 2004

**Abstract**

The present study analyzes the catalytic behavior of Metal/HZSM5–$Al_2O_3$ catalysts (Metal = Ni, Mo or Pt), in the hydroconversion of a model mixture of *n*-heptane–benzene–toluene. A systematic study was performed to understand the activity and selectivity properties of the catalysts, and to analyze the relationship between the acid/metal balance of the catalysts and the main reaction paths, with impact on octane enhancement and liquid yield. Finally, the results obtained with the model mixture are contrasted with those obtained using a real hydrotreated FCC gasoline with less than 1.0 wt.% olefins.

The main reaction pathways for octane enhancement over monofunctional HZSM5($x$)–$Al_2O_3$ catalysts are isomerization and cracking of *n*-heptane, dimerization–cracking of *n*-heptane, and aromatic alkylation reactions, being the last two routes the most important for producing high octane hydrocarbons. In the presence of a strong metallic function isomerization and cracking of *n*-heptane, and aromatics hydrogenation reactions are the main routes. In this case octane enhancement is achieved mainly through isomerization reactions. These results indicate that although there is an opposite trend between the RON and liquid yield of the product, it is possible to increase the barrel-octane with the catalysts used here. When a hydrotreated FCC gasoline was used as the feed, the observed changes in RON and liquid yield when the process variables were changed, followed similar trends to those of the synthetic feed, although less drastic. A detailed analysis (PIONA) of the product distribution indicates that for FCC gasoline RON enhancement comes mainly from cracking and isomerization of paraffins and naphthenes, and from the formation of alkylated aromatics. The main reaction pathways in the hydroconversion process leading to higher RON with the synthetic mixture and the real feed are similar.


*Keywords:* Hydroconversion; *n*-Heptane–benzene–toluene; Octane enhancement; HZSM5; Ni; Mo; Pt; Reaction pathways

## 1. Introduction

The study of hydroconversion processes over bifunctional metal/acid catalysts is of great industrial importance because these processes are one of the ways to improve the quality of the transportation fuels obtained from different petroleum cuts. In the past, most hydroconversion studies were performed with single molecules like *n*-heptane [1–3]. Even in these simple studies a great number of reactions take place. Not surprisingly, because of the complexity of the problem, only few studies have been performed using complex feedstocks, which are more representative of the processes occurring with real feeds [4,5]. In this case, the number of main reaction routes leading to the observed product distributions increases substantially.

This work analyzes the hydroconversion of a complex hydrocarbon mixture constituted by a paraffin (*n*-heptane 80 vol.%), and two aromatics (benzene 10 vol.% and toluene 10 vol.%). Although not fully representative, because of the lack of isoalkanes and naphthenes, the hydroconversion results of this mixture are contrasted with those obtained with a hydrotreated FCC gasoline, which has lost octane during the hydrodesulfurization step, because of the hydrogenation of about 99% of the olefins. In fact,

* Corresponding author. Tel.: +52 5 55622 53 66; fax: +52 5 55622 53 66.
*E-mail address:* hogoro@netscape.net (H. González).

0920-5861/$ – see front matter © 2004 Elsevier B.V. All rights reserved.
doi:10.1016/j.cattod.2004.07.032

several commercial processes have been proposed to hydrotreat the FCC gasoline stream without loss of octane [6]. They consist of two main reaction steps, deep hydrodesulfurization followed by a hydroconversion step in which the octane is recovered or enhanced. It is the hydroconversion step, which has been the least studied especially regarding the catalyst formulation.

It is well known that metal and acid sites are active in hydrocarbon transformations through different reaction mechanisms. Catalyst reactivity and selectivity is related to its acid/metal functionality ratio balance, which should be appropriate for the composition of the fuel fraction to be processed. By carefully balancing the metal and acid functions is possible to generate a synergism leading to a significant increase in reaction rate and a change in product distribution [7]. Studies concerning how different catalyst formulations affect the activity and selectivity of this process are scarce [8,9].

The present study analyzes the catalytic behavior of Metal/HZSM5–$Al_2O_3$ catalysts (Metal = Ni, Mo, and Pt), concerning the activity, selectivity, and reaction pathways, in the hydroconversion of a model complex mixture of hydrocarbons (*n*-heptane–benzene–toluene). The main reaction routes with impact on octane enhancement and liquid yield will be analyzed and discussed in terms of the catalysts characterization results (XRD, textural properties, TPD-$NH_3$). Finally, the results obtained with the model mixture are contrasted with those obtained using a real feed, hydrotreated FCC gasoline.

## 2. Experimental

### 2.1. Catalysts preparation

The catalysts were prepared with a commercial HZSM5 zeolite (Zeolyst, $SiO_2/Al_2O_3$ molar ratio = 80). The incorporation of the zeolite (10 wt.%) to the alumina matrix was achieved by using boehmite (Catapal B) as binder. Hereafter the monofunctional catalysts will be referred as HZSM5(*x*)–alumina where *x* is the weight percent of zeolite in the catalysts. The metallic components were incorporated to the HZSM5(*x*)–alumina by pore volume impregnation. Aqueous solutions of nickel nitrate, ammonium heptamolybdate, and chloroplatinic acid were used in the appropriate concentrations to obtain different catalysts with metal contents of 1, 3.5 wt.% Ni; 3, 9 wt.% Mo; and 0.3, 0.5 wt.% Pt. After impregnation the catalysts were dried at 393 K and calcined at 773 K during 4 h for the Ni and Mo catalysts and at 673 K during 4 h for the Pt-based catalysts.

### 2.2. Catalytic experiments

The catalytic experiments were performed in a tubular stainless steel reactor. The feed (mol%): *n*-heptane (70.66%)–benzene (15.62%)–toluene (13.29%) was added continuously by a Milton Roy high-pressure pump. Mass flow controllers were used to control the flow of hydrogen (100 ml/min) and nitrogen (60 ml/min). The reaction was conducted at 588 K and 28 $kg/cm^2$, using a liquid hourly space velocity (LHSV) of 2.5 $h^{-1}$, and a molar hydrogen/hydrocarbon ratio of 2. The liquid reaction products were analyzed by gas chromatography using a 50-m PONA capillary column. Prior to the catalytic test, the catalysts were pre-treated with nitrogen (588 K, 1 h), and then either with hydrogen at 723 K during 4 h (reduction pre-treatment) or with a $CS_2$ (3.5 wt.%)/cyclohexane mixture at 573 K, using hydrogen has carrier (100 ml/min) during 4 h (sulfidation pre-treatment).

### 2.3. Catalysts characterization

The X-ray powder diffraction patterns were recorded in the $2^\circ \leq 2\theta \leq 70^\circ$ range in a Siemens D5000 diffractometer, using Cu Kα radiation, a goniometer speed of 1.0°/min and a graphite monochromator. BET surface areas were determined by nitrogen physisorption at 77 K in a Micromeritics ASAP 2000 apparatus. The total acid site density and acid strength distribution of the catalysts were measured by temperature-programmed desorption of ammonia (TPD) in a RIG-100 catalyst characterization apparatus equipped with a continuous quartz tubular reactor. The sample (500 mg) was housed into the reactor, then pre-treated in flowing air while heating at 10 K/min to 773 K, and maintaining at this temperature for 1 h. In a second step the samples were pre-treated in a helium stream at the same temperature for 1 h. After cooling the sample to room temperature, it was ammonia-saturated with a 15% $NH_3$/He stream (30 ml/min). Then, the ammonia was desorbed by using a linear heating of 5 K/min to 773 K recording continuously the temperature and detector signals. The area under the curve was integrated to determine the relative total acidity of the catalysts.

## 3. Results and discussion

### 3.1. Characterization of the catalysts

Analysis of the chemical phases present in the catalysts, their textural and acid properties are relevant for understanding the behavior of Metal/HZSM5(*x*)–alumina catalysts in the hydroconversion process. Characterization of the catalysts was performed in order to determine the effect of metal incorporation to HZSM5(10)–$Al_2O_3$ on the textural properties ($N_2$ physisorption), crystalline structure (XRD), and acid properties (TPD-$NH_3$) of the final calcined bifunctional catalysts.

#### 3.1.1. X-ray diffraction

The XRD patterns of different Metal/HZSM5(10)–alumina samples are shown in Fig. 1. The pattern of the

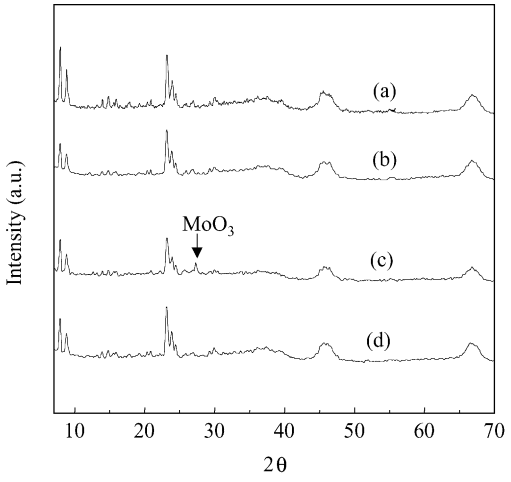


Fig. 1. X-ray diffraction patterns of samples: (a) HZSM5(10)–alumina, (b) Ni(1%)/HZSM5(10)–alumina, (c) Mo(9%)/HZSM5(10)–alumina, and (d) Pt(0.3%)/HZSM5(10)–alumina.

monofunctional HZSM5(10)–alumina catalyst, included for comparison purposes (Fig. 1a), presents the main diffraction lines associated with HZSM5 and γ-alumina (matrix). The incorporation of Mo(3%), Pt(0.3%) or Ni(1%) to HZSM5–alumina causes a small decrease in the intensity of the main diffraction lines present in the monofunctional catalyst, which results from a dilution effect of the zeolite in the Metal–zeolite system. No diffraction lines corresponding to Pt or Ni phases are detected indicating good dispersion of these metals. In contrast, the XRD pattern for the Mo(9%) sample shows an additional reflection located at $2\theta = 27.34^\circ$, which corresponds to the main reflection of $MoO_3$ (JCPDS card 35-609), the remaining diffractogram features agree well to those observed for the HZSM5–alumina sample.

### 3.1.2. Textural properties

The textural properties of Metal/HZSM5(10)–alumina samples in the oxide state are shown in Table 1. Catalysts with low metal loading (Ni and Pt catalysts, and Mo 3 wt.%) exhibit textural properties similar to those of the HZSM5–alumina support. However, the incorporation of a higher Mo loading (9%) causes a decrease in surface area (15%) and pore volume (18%). This result is due to some pore blockage and is well in line with the large $MoO_3$ particles observed by XRD in this sample. Additional experiments (not shown), indicated that some pore blockage also occurs at 6 wt.% Mo. In a previous FT-IR study on the interaction of *n*-heptane, benzene, and toluene with Mo/ZSM5, we showed that Mo is located mainly on the external zeolite surface, therefore with almost no interaction with the strong internal zeolite acid sites [9]. At Mo contents of 6 wt.%, *n*-heptane can penetrate and interact with the internal hydroxyls while benzene and toluene are not able to reach the internal OH's because the Mo species hinder the molecular diffusion into the zeolite cavities.

Table 1
Textural properties of Metal/HZSM5(10)–alumina catalysts

| Metal (wt.%) | BET area ($m^2$/g) | Pore volume ($cm^3$/g) |
|---|---|---|
| 0% | 271 | 0.44 |
| 1% Ni | 274 | 0.43 |
| 3.5% Ni | 259 | 0.42 |
| 3% Mo | 271 | 0.42 |
| 9% Mo | 234 | 0.36 |
| 0.3% Pt | 267 | 0.42 |
| 0.5% Pt | 263 | 0.41 |

Table 2
$NH_3$-TPD acidity of Metal/HZSM5(10)–alumina catalysts for different temperature regions

| | $T_{room}$–473 K | 473–573 K | 573–$T_{final}$ K | Total |
|---|---|---|---|---|
| μmol $NH_3$/g | | | | |
| No metal | 210.2 | 83.5 | 150.9 | 444 |
| Ni(1%) | 209.7 | 80.9 | 142.0 | 432.6 |
| Ni(3.5%) | 196.9 | 80.7 | 130.0 | 408.2 |
| Mo(3%) | 228.9 | 69.4 | 122.7 | 420.8 |
| Mo(9%) | 150.9 | 61.0 | 85.1 | 298 |
| Pt(0.3%) | 234.2 | 85.9 | 151.9 | 471.7 |
| Pt(0.5%) | 225.2 | 80.5 | 144.7 | 450 |

### 3.1.3. $NH_3$-TPD

The quantitative analysis of the $NH_3$-TPD patterns for different catalyst samples is presented in Table 2. For convenience the TPD patterns were divided in three main regions, characterizing different types of acidity (weak: $T_{room}$–473 K; medium: 473–573 K; and strong: 573–$T_{final}$).

The incorporation of nickel (1 and 3.5 wt.%) to the monofunctional catalyst leads to a small decrease (5 and 13%, respectively) in the strong acidity of the calcined catalysts, whereas weak and medium acidity do not suffer important changes. The decrease in the number of strong acid sites for the Ni-based samples could be associated with the ion exchange process, which occurs between the $Ni^{2+}$ species and Brönsted acid sites of the zeolite. This process that occurs during the impregnation of the catalysts eliminates two acid sites per each $Ni^{2+}$ cation, diminishing the number of Brönsted acid sites [10,11].

The samples impregnated with 0.3 and 0.5 wt.% of Pt showed minor changes in their acid properties, only a small increase in weak and medium acidity was observed. This acidity increase was related to small amounts of $Cl^-$ remaining in the alumina matrix from the impregnation with $H_2PtCl_6$, which gives rise to stronger acid sites [12]. The greater amount of weak acid sites was due to an increase in the amount of physisorbed $NH_3$, possibly related also to the presence of $Cl^-$ in the sample.

Compared with the monofunctional catalyst, the number of medium and strong acid sites of Mo(3%)/HZSM5–alumina decreases about 17 and 18%, respectively, indicating some interaction of the Mo species with the strong internal acid sites of the zeolite. For the catalyst with 9 wt.% Mo the acidity drops even more.

### 3.2. Catalytic experiments

Metals with three different levels of hydrogenating power (Ni, Mo or Pt) were used in this study in order to modify the acid/metal balance of the bifunctional catalysts. In all reaction experiments a complete product distribution analysis was made. Tables 3 and 4 show typical results obtained with the pre-sulfided Ni(3.5%)/HZSM5–$Al_2O_3$ catalyst. In general it was observed that the main reaction products lighter than heptane are alkanes with predominance of propane, *n*-butane, isobutane, pentane, and hexane. Only small amounts of light olefins are detected, with preponderance of propene, butanes, and 2-methyl-2-butene. Some branched heptane isomers and small amounts of heptenes are also found. Among the products heavier than the reactants, a clear predominance is found for alkyl-benzenes and alkyl-toluenes. Detectable amounts of alkanes higher than heptane ($>C_7$) are also found, these higher paraffins can be the result of aliphatic alkylation reactions between olefinic fragments and carbenium ions adsorbed on the catalyst surface, both of them produced during heptane cracking.

Table 3
Typical product distribution of the $C_5$+ liquid fraction for the pre-sulfided Ni(3.5%)/HZSM5–$Al_2O_3$ catalyst

| Product | mol% | Product | mol% |
|---|---|---|---|
| Isopentane | 1.95 | $C_8$ cycloparaffins | 0.27 |
| 2-Methyl-1-butene | 0.08 | 3-Methylheptane | 0.13 |
| *n*-Pentane | 3.58 | $C_8$ olefins | 0.04 |
| Cyclopentene | 0.02 | *n*-Octane | 0.13 |
| 2-Methyl-2-butene | 0.17 | Ethylbenzene | 0.20 |
| 2,2-Dimethylbutane | 0.01 | *m*-Xylene | 0.12 |
| Cyclopentane | 0.02 | *p*-Xylene | 0.08 |
| 2,3-Dimethylbutane | 0.09 | $C_9$ isoparaffins | 0.15 |
| 2-Methylpentane | 0.88 | *o*-Xylene | 0.04 |
| 3-Methylpentane | 0.37 | *n*-Nonane | 0.02 |
| $C_6$ olefins | 0.07 | $C_9$ cycloparaffins | 0.09 |
| *n*-Hexane | 1.41 | Isopropylbenzene | 1.85 |
| 2,2-Dimethylpentane | 0.01 | *n*-Propylbenzene | 1.07 |
| Methylcyclopentane | 0.12 | *m*-Ethyltoluene | 0.22 |
| 2,4-Dimethylpentane | 0.02 | *p*-Ethyltoluene | 0.15 |
| 2,2,3-Trimethylbutane | Trace | 1,3,5-Trimethylbenzene | 0.02 |
| Benzene | 12.99 | $C_{10}$ isoparaffins | 0.52 |
| 3,3-Dimethylpentane | 0.01 | *o*-Ethyltoluene | 0.02 |
| Cyclohexane | 0.22 | 1,2,4-Trimethylbenzene | 0.06 |
| 2-Methylhexane | 0.45 | $C_{10}$ cycloparaffins | 0.03 |
| 2,3-Dimethylpentane | 0.10 | Isobutylbenzene | 0.12 |
| Dimethylcyclopentanes | 0.24 | 1,2,3-Trimethylbenzene | 0.34 |
| 3-Methylhexane | 0.45 | 1-Methyl-4-isopropylbenzene | 0.32 |
| 3-Ethylpentane | 0.08 | $C_{11}$ isoparaffins | 0.11 |
| $C_7$ Olefins | 0.15 | 1-Methyl-2-isopropylbenzene | 0.03 |
| *n*-Heptane | 52.69 | 1,3-Diethylbenzene | 0.02 |
| Methylcyclohexane | 0.53 | 1-Methyl-3-propylbenzene | 0.59 |
| 2,2-Dimethylhexane | 0.03 | 1-Methyl-4-propylbenzene | 0.32 |
| Ethylcyclopentane | 0.05 | *n*-Butylbenzene | 0.41 |
| 2,5-Dimethylhexane | 0.01 | 1-Methyl-2-propylbenzene | 0.05 |
| 2,4-Dimethylhexane | 0.01 | 1,3-Dimethyl-4-ethylbenzene | 0.01 |
| 3,3-Dimethylhexane | Trace | 1,2-Dimethyl-4-ethylbenzene | 0.06 |
| Toluene | 12.78 | 1-Methyl-3-terbutylbenzene | 0.03 |
| 2,3-Dimethylhexane | 0.06 | 1,2-Dimethyl-3-ethylbenzene | 0.14 |
| 2-Methylheptane | 0.08 | 1,2,4,5-Tetramethylbenzene | 0.01 |
| 4-Methylheptane | 0.05 | 1,2,3,5-Tetramethylbenzene | 0.07 |
| 3,4-Dimethylhexane | 0.01 | 1,2,3,4-Tetramethylbenzene | 0.22 |
| | | Unidentified | 2.15 |
| | | Liquid yield (%) | 80.2 |
| | | RON of the liquid product | 35.1 |

Table 4
Typical gas product distribution for pre-sulfided Ni(3.5%)/HZSM5–$Al_2O_3$ catalyst

| Product | mol% |
|---|---|
| Ethane | Trace |
| Ethene | Trace |
| Propene | 2.54 |
| Propane | 52.97 |
| Isobutane | 20.60 |
| 1-Butene + isobutylene | 1.01 |
| *n*-Butane | 22.82 |
| *t*-2-Butene | Trace |
| *c*-2-Butene | 0.06 |

#### 3.2.1. Metal/alumina catalysts

To assess what reactions were possible in the absence of zeolite, some experiments were conducted over metal/alumina catalysts after pre-treatments of reduction and sulfidation. The results, presented in Table 5, indicate that, at the operating conditions of this study, all the samples without zeolite do not catalyze the isomerization and alkylation reactions. The main reactivity of the reduced Ni and Pt catalysts was associated with some *n*-heptane cracking and aromatic hydrogenation reactions. Upon sulfidation these catalysts showed a much lower hydrogenating activity. As expected the hydrogenation activity of the Pt catalysts was much higher than for Ni or Mo. In fact, Mo catalysts only showed significant activity in the cracking reactions and no activity in the hydrogenation of aromatics. The pre-sulfided Mo(3%)/alumina catalyst showed the highest conversion of *n*-heptane (about 7%) leading mainly to light hydrocarbons. With this catalyst, the conversion of aromatics was similar to that observed for *n*-heptane (6–8%). The product distribution analysis showed absence of hydrogenation products and formation of alkyl-aromatics and $C_{10}$+ products. The transformation of aromatics over sulfided Mo(3%)/alumina was thus related to reactions such as alkylation [13] and possibly some aromatic recombination reactions leading to coke precursors [14].

#### 3.2.2. Metal/HZSM5–alumina catalysts

For each reaction experiment a detailed product analysis was made. From these analyses a lumped product distribution was also calculated. Table 6 presents lumped product distributions for the different catalysts. Reactants conversions and selectivity for the monofunctional and bifunctional catalysts are also shown. The monofunctional catalyst, taken as the reference with zero metal, presents a high conversion of reactants (*n*-heptane, benzene, and toluene). With this catalyst the most important products were those coming from cracking ($C_4-$) and alkylation ($C_8$+) reactions. A significant amount of $C_5$ and $C_6$ products

Table 5
Catalytic behavior of Metal/alumina catalysts under reduction or sulfidation pre-treatment

| | Metal($x$%)/$Al_2O_3$ (wt.%) | | | | | | |
|---|---|---|---|---|---|---|---|
| | Ni(1) | | Ni(3.5) | Mo(3) | | Pt(0.3) | |
| | Sulfidation | Reduction | Reduction | Sulfidation | Reduction | Sulfidation | Reduction |
| $C_4-$ (wt.%) | 1.0 | 4.6 | 5.5 | 7.1 | 1.4 | 5.1 | 5.3 |
| $Y_{CHA}$[a] (%) | – | – | 76.1 | – | – | 8.2 | 76.2 |
| $Y_{MCHA}$[b] (%) | – | 0.2 | 64.6 | – | – | 9.5 | 58.5 |
| $X_{Bz}$ (%) | 0 | 0 | 76.2 | 6.9 | 2.1 | 8.5 | 76.0 |
| $X_{nC7}$ (%) | 1.3 | 6.5 | 5.6 | 6.6 | 0.6 | 5.2 | 5.8 |
| $X_{Tol}$ (%) | 0.2 | 3.6 | 65.1 | 8.3 | 3.6 | 10.0 | 58.7 |

CHA, cyclohexane; MCHA, methylcyclohexane; $X_{Bz}$, benzene conversion; $X_{nC7}$, *n*-heptane conversion; $X_{Tol}$, toluene conversion. Sulfidation and reduction are pre-treatments.

[a] $Y_{CHA}$ = (mol CHA/mol Bz) × 100.

[b] $Y_{MCHA}$ = (mol MCHA/mol Tol) × 100.

constituted mainly by paraffins, and isoparaffins was also detected. Since the $C_1/C_6$ and $C_2/C_5$ ratios (not shown) were small, it can be said that the two former groups of products came from dimerization–cracking reactions. The $C_7$ group is mainly the result of *n*-heptane isomerization reactions. With this catalyst the olefins to paraffins molar ratio in the product was in general small (<0.02), as a result of the high hydrogen transfer activity of the zeolite.

*3.2.2.1. Effect of the type of metal and pre-treatment of the catalysts.*

*3.2.2.1.1. Pre-reduced catalysts.* The incorporation of a metallic function of increasing hydrogenating power (Ni and Pt) causes some important changes in the product distribution. Compared with the metal-free catalyst, the reduced Ni(3.5%) catalyst (low hydrogenating function) displays an important decrease in *n*-heptane conversion (9.1%) as well as a lowering of the production of alkyl-aromatics, groups $C_8$, $C_9$, and $C_{10}$ (4 mol%). With a high hydrogenating function, Pt(0.3%) catalyst, the production of alkyl-aromatics is suppressed but the production of *n*-heptane isomers, light hydrocarbons ($C_4-$), and products from aromatics hydrogenation reactions is substantially enhanced. With the Pt catalyst the conversion of reactants is significantly greater than with the Ni or Mo catalyst.

From the above results it becomes clear that the characteristics of the particular metal component in the catalyst alter in different ways the product distribution of the reaction. To stress more this point, column 5 in Table 6 presents the results obtained with a catalyst containing

Table 6
Effect of the metal function and pre-treatment over the activity and selectivity of Metal/HZSM5(10)–alumina catalysts

| | Metal($x$%)/HZSM5(10)–$Al_2O_3$ | | | | | | |
|---|---|---|---|---|---|---|---|
| | No metal | Ni(3.5) | | Mo(3) | | Pt(0.3) | |
| | | Reduction | Sulfidation | Reduction | Sulfidation | Reduction | Sulfidation |
| mol% | | | | | | | |
| $C_4-$ | 44.23 | 39.60 | 37.80 | 37.50 | 43.63 | 61.50 | 43.16 |
| $C_5$ | 4.14 | 3.74 | 3.64 | 4.21 | 5.10 | 0.41 | 1.76 |
| $C_6$ | 2.24 | 2.31 | 1.99 | 1.83 | 2.68 | 5.84 | 1.04 |
| $C_7$ | 1.36 | 1.42 | 1.22 | 0.91 | 1.27 | 8.89 | 1.36 |
| $C_8$ | 0.90 | 0.23 | 0.58 | 0.93 | 0.99 | 0.02 | 0.11 |
| $C_9$ | 2.66 | 1.37 | 2.36 | 3.23 | 3.37 | 0.00 | 0.85 |
| $C_{10}$ | 2.06 | 1.01 | 1.77 | 2.31 | 2.49 | 0.00 | 0.41 |
| $C_{10}+$ | 0.93 | 0.24 | 0.64 | 0.97 | 0.94 | 0.00 | 0.00 |
| Benzene | 7.57 | 9.19 | 8.28 | 7.71 | 8.43 | 2.73 | 9.99 |
| *n*-heptane | 26.53 | 32.05 | 33.58 | 32.13 | 22.71 | 17.47 | 31.83 |
| Toluene | 7.38 | 8.83 | 8.15 | 8.26 | 8.38 | 3.13 | 9.49 |
| Conversion (%) | | | | | | | |
| *n*-Heptane | 52.72 | 43.62 | 42.35 | 45.35 | 59.56 | 64.71 | 42.60 |
| Benzene | 38.97 | 26.92 | 35.69 | 40.68 | 33.93 | 75.08 | 18.49 |
| Toluene | 30.09 | 17.41 | 25.64 | 25.30 | 22.78 | 66.35 | 9.05 |
| $\gamma_t$ (%) | 8.21 | 3.53 | 7.45 | 11.06 | 9.73 | – | 1.92 |
| $\gamma_{t+dc}$ (%) | 20.57 | 23.02 | 21.31 | 20.43 | 22.80 | 32.96 | 14.07 |
| Isoheptanes (mol%) | 0.78 | 0.92 | 0.69 | 0.54 | 0.88 | 4.83 | 1.04 |

Reduction and sulfidation are pre-treatments.

molybdenum (Mo(3%)/HZSM5(10)–alumina) in a reduced state. With the Mo catalyst one obtains an *n*-heptane conversion slightly higher than with the Ni catalyst whereas the amount of cracking ($C_4-$ to $C_6$) and isomerization ($C_7$) products are similar. The main difference with respect to the Ni catalyst is that Mo catalyst promotes more the alkylation reactions. This feature is even more notorious if one compares Mo and Pt catalysts because with the later the alkylation reactions are almost completely suppressed. Mo catalyst in fact behaves close to the monofunctional catalyst but with less production of light products (6.5 mol%).

These results clearly indicate that one of the functions of the metallic component in the catalyst is the hydrogenation of the olefinic intermediaries produced during *n*-heptane cracking [15]. These olefinic intermediaries, which participate in the production of alkylated aromatics, are hydrogenated on the metallic sites of the catalyst. This explains in part the differences in product distribution between Ni and Pt based catalysts. In fact, when the hydrogenating function is strong enough, the production of alkylated products may be completely suppressed, as indeed is observed in the case of the Pt-containing catalyst (see Table 6). For the Ni catalyst, with a much lower hydrogenating function, the production of alkyl-aromatics was substantially higher. Therefore, the drastic change in selectivity observed for the two catalysts is due to a modification in the balance of the acid and hydrogenating functions. In the case of the Pt-based catalyst, the acid/hydrogenating functions balance is shifted in favor of the *n*-heptane isomerization route. At the same time, hydrogenation of the olefinic intermediaries and hydrocracking of *n*-heptane over the metallic sites of the catalyst are also enhanced, leading to a high production of light products.

*3.2.2.1.2. Pre-sulfided catalysts.* The sulfidation treatment also changes conversion and product distribution. Under sulfidation *n*-heptane conversion with the Ni catalyst remains practically the same while with the Mo catalyst is significantly enhanced (7 mol% with respect to the monofunctional catalyst). With the Pt based catalyst, the sulfidation pre-treatment leads to a substantial decrease in the production of light products (about 18 wt.%) and a relatively important production of alkyl-aromatics (≈1.5 mol%), with respect to the pre-reduced catalyst. Also, with the sulfidation pre-treatment, *n*-heptane isomerization and hydrogenation of aromatics are substantially decreased. Upon sulfidation, the Ni-based catalyst shows, although to a lower extent, essentially the same behavior as the Pt-based catalyst. In this case the sulfidation pre-treatment leads to a decrease of about 2 wt.% in the production of light products, and to an increase in the production of alkyl-aromatics. A decrease in the direct isomerization of *n*-heptane is also observed. The reduced Mo catalyst produces approximately the same amount of alkyl-aromatics than the Mo catalyst in its sulfided state.

The pre-sulfided Mo(3%)/HZSM5–alumina catalyst showed an important increase in the catalytic activity when compared with the monofunctional catalyst. This result is mainly associated with the relatively high hydrogenating–dehydrogenating capacity of the sulfided Mo phase, which promotes the bifunctional hydroconversion mechanism. In addition, the production of light hydrocarbons was about 3 wt.% lower than that obtained with the monofunctional catalyst (at the same *n*-heptane conversion) while the production of $C_5$–$C_7$ isomers increased about 1 wt.% and the production of alkyl-aromatics $C_8$ decreased about in the same percentage. In the literature [16] there is some evidence that the Mo species are capable of catalyzing some isomerization reactions, thus the observed increase in the production of $C_5$–$C_7$ isomers could be associated with the presence of these species. Therefore, as a consequence of the higher catalytic activity, the lower production of light hydrocarbons and the higher production of $C_5$–$C_7$ isomers, the gain in barrel-octane for the low Mo-content catalyst (3 wt.%) was the highest when compared with the Ni or Pt based catalysts.

The above observations in the hydroconversion of the feed mixture (*n*-heptane–benzene–toluene) are in line with the modifications in the acid/hydrogenating function balance induced by changes of the type and state of the metal in the catalyst formulation. In general, the sulfidation pre-treatment reduces the hydrogenating power of the metallic phase and, at the same time, increases the acid function due to the creation of new acid sites, thus leading to a behavior closer to that of the acid monofunctional catalyst.

In order to rationalize better the behavior of the different catalysts, we defined two new selectivity indexes, calculated from the carbon balance of the complete product distribution for each case (not shown). These indexes are included in Table 6. We defined the isomerization index ($\gamma_{i+dc}$) as the percent of the *n*-heptane carbon moles that appear as $C_5$–$C_7$ products. This index encompasses the transformation of *n*-heptane via isomerization and dimerization–cracking leading to $C_7$ isomers and $C_5$–$C_6$ fractions, respectively. In a similar way the trapping index ($\gamma_t$) is defined as the percent of the *n*-heptane carbon moles captured by aromatics and which after reaction appear as alkyl groups in the $C_8$+ products.

With the monofunctional catalyst the $\gamma_t$ index was approximately 8% whereas the $\gamma_{i+dc}$ index was 20.5. These values indicate that a greater proportion of the carbons present in the *n*-heptane feed appear as $C_5$–$C_7$ in the products. About 8% of the carbons in *n*-heptane end up as part of alkyl substitutes in the aromatics. This is reflected in the significant conversions of benzene (38.97%) and toluene (30.1%). The rest of the *n*-heptane (47%) mainly transforms to light products ($C_4-$).

These indexes, used here for the first time, also help to visualize more clearly the behavior of the catalysts, for example it is easy to see that in their reduced and sulfided states the Mo catalyst promotes the alkylation more than the Ni or Pt catalysts, that in general sulfidation promotes the alkylation reactions and that with the reduced Pt catalyst, 32% of the *n*-heptane end up as isomers while non ends up in the alkyl groups of alkyl-aromatics ($C_8$+). The remaining

Table 7
Effect of the metal loading over the product distribution, activity, and selectivity

| | Metal($x$%)/HZSM5(10)–$Al_2O_3$ | | | | | | |
|---|---|---|---|---|---|---|---|
| | No metal | Ni(1) | Ni(3.5) | Mo(3) | Mo(9) | Pt(0.3) | Pt(0.5) |
| mol% | | | | | | | |
| $C_4-$ | 44.23 | 39.12 | 37.80 | 43.63 | 39.54 | 43.16 | 53.98 |
| $C_5$ | 4.14 | 3.58 | 3.64 | 5.10 | 4.24 | 1.76 | 1.73 |
| $C_6$ | 2.24 | 2.00 | 1.99 | 2.68 | 2.54 | 1.04 | 0.88 |
| $C_7$ | 1.36 | 0.94 | 1.22 | 1.27 | 0.81 | 1.36 | 1.57 |
| $C_8$ | 0.90 | 0.63 | 0.58 | 0.99 | 0.28 | 0.11 | 0.13 |
| $C_9$ | 2.66 | 2.65 | 2.36 | 3.37 | 2.35 | 0.85 | 0.55 |
| $C_{10}$ | 2.06 | 2.02 | 1.77 | 2.49 | 1.42 | 0.41 | 0.24 |
| $C_{10}+$ | 0.93 | 0.43 | 0.64 | 0.94 | 0.20 | 0.00 | 0.00 |
| Benzene | 7.57 | 7.73 | 8.28 | 8.43 | 10.01 | 9.99 | 9.95 |
| *n*-Heptane | 26.53 | 32.96 | 33.58 | 22.71 | 28.82 | 31.83 | 21.90 |
| Toluene | 7.38 | 7.94 | 8.15 | 8.38 | 9.77 | 9.49 | 9.08 |
| Conversion (%) | | | | | | | |
| *n*-heptane | 52.72 | 43.04 | 42.35 | 59.56 | 49.29 | 42.60 | 57.32 |
| Benzene | 38.97 | 39.59 | 35.69 | 33.93 | 20.31 | 18.49 | 12.31 |
| Toluene | 30.09 | 27.06 | 25.64 | 22.78 | 8.59 | 9.05 | 5.94 |
| $\gamma_t$ (%) | 8.21 | 7.76 | 7.45 | 9.73 | 6.56 | 1.92 | 1.05 |
| $\gamma_{i+dc}$ (%) | 20.57 | 19.82 | 21.31 | 22.80 | 22.12 | 14.07 | 11.84 |
| Isoheptanes (mol%) | 0.78 | 0.60 | 0.69 | 0.88 | 0.69 | 1.04 | 1.18 |

Pre-sulfided Metal/HZSM5(10)–alumina catalysts.

68% of the *n*-heptane conversion goes mainly to light products. The enhanced value of the $C_6$ and $C_7$ products with the Pt catalyst are due to the production of $C_6$ and $C_7$ hydrogenated products from benzene and toluene.

The pre-reduced Mo-based catalyst presented a different behavior compared with the Ni or Pt based catalysts. This catalyst showed a 3% increase in the trapping index ($\gamma_t$) while the isomerization–dimerization index ($\gamma_{i+dc}$) was about 20%. In fact the reduction pre-treatment does not modify significantly the acid/metal balance of this catalyst, probably because of the difficulty to reduce completely the supported Mo species, as reported in the literature [17].

*3.2.2.2. Effect of the metal loading.* To study the effect of the metal loading, two different concentrations of Ni, Mo, and Pt were incorporated to the monofunctional catalyst and tested in the hydroconversion reaction using a sulfidation pre-treatment. The results from these tests are presented in Table 7, where they are compared with the results obtained with the monofunctional metal-free catalyst.

An increase in the number of metallic sites achieved by using higher metal loading, alters not only the acid/metal balance of the catalyst but also some physicochemical properties such as the surface area and pore volume, and also in some cases the number of acid sites are significantly modified due to the blockage of some pores by the metallic phase. Our results show that for the catalysts with low metal loading (Pt and Ni catalysts) the textural properties remain similar to the metal-free catalyst. In contrast, for the Mo catalysts with high metal loading the surface area and pore volume drop significantly (see Table 1). Concerning the acid properties, we observe a slight decrease in the number of acid sites for Ni (1 and 3.5%) and a significant one for the Mo(9%) catalyst (see Table 2).

The changes in metal loading also altered the activity and selectivity of the catalysts. For the Pt catalysts in which the metal loading is small and do not alter the textural and acid properties of the catalyst, the observed changes in reactivity (increase in *n*-heptane conversion and decrease in aromatics conversion) are the result of an enhanced metallic function. The decrease in the conversion of aromatics is the result of a high rate of hydrogenation of the olefins produced from heptane cracking. The increase in Pt loading also produces an important increase in the hydrocracking reactions, as a result of the operation of a bifunctional mechanism of paraffin's hydrocracking, and possibly to hydrogenolysis reactions. Thus, we observe a 10 mol% increase in the production of light products. In the case of Mo catalysts the changes in product distribution with metal loading come from a change in the metallic/acid balance but also from the significant changes observed in surface area and acidity of the catalyst.

The increase in the Ni loading, do not alter much the product distribution because at the loadings used, the textural and acid properties are not greatly affected and the hydrogenating capacity does not change significantly.

More drastic changes in the catalytic properties were observed for the Mo-based catalysts. This is understandable since the metal loading was approximately an order of magnitude higher compared with the Ni or Pt samples. A change in the Mo loading from 3 to 9% leads to a decrease in *n*-heptane conversion, along with a significant decrease in the conversion of benzene (13%) and toluene (14%), at the same time the selectivity to high-octane hydrocarbons drops

Table 8
Characteristics of the hydrotreated FCC gasoline

| | |
|---|---|
| Nominal boiling range (K) | 355–477 |
| Specific gravity (g/cm$^3$) | 0.805 |
| Total sulfur (ppm) | 147 |
| Nitrogen (ppm) | 18 |
| Research octane number (RON) | 84.8 |

significantly. This behavior resulted, as explained before, from the partial blockage of the zeolite channels entrances by $MoO_3$ particles, leading to an inhibition in the production of alkylated aromatics [9]. In fact as the characterization results showed, for Mo catalysts with high metal loading, surface area, and pore volume drops significantly (see Table 1). The observed increase in catalytic activity for the low Mo content catalyst probably comes from the operation of the bifunctional hydroconversion mechanism and to a lower extent by the increase in acidity by the Mo–S–H groups [18].

All these results are clearly reflected in the $\gamma_{i+dc}$ and $\gamma_t$ indexes. For the Ni(3.5%) catalyst the $\gamma_{i+dc}$ index increased slightly (1.5%) while the trapping index ($\gamma_t$) dropped approximately 0.3% with reference to the Ni(1%) sample. With the Mo catalyst the $\gamma_{i+dc}$ index remained approximately constant with the metal loading but the trapping index dropped from 10 to 6.5% as the metal loading was increased from 3 to 9% Mo. In contrast in the case of Pt-based catalysts both indexes, $\gamma_{i+dc}$ and $\gamma_t$, decrease with metal loading (0.9 and 2.2, respectively).

### 3.2.3. Hydroconversion of hydrotreated FCC gasoline

Hydroconversion experiments were also performed with a real hydrotreated FCC gasoline feed. The main characteristics of the FCC gasoline used in the catalytic experiments are presented in Table 8. Since the feed contained 147 ppm of sulfur, a sulfidation pre-treatment was given to the catalysts.

In Table 9 the product distribution obtained with pre-sulfided Ni and Pt-based catalysts is presented along with the results of RON and liquid yield. The gain in RON obtained with the Ni-based catalysts and the monofunctional catalyst is quite similar (about 3 units), while the liquid yield is slightly higher for the Ni-based catalyst. As show in Table 9, the most important change in product distribution is observed for the isoparaffins group, which presents an increase of 2 and 3 wt.% for the Ni and Pt based catalyst, respectively. Regarding the aromatics group, it only showed a small increase for the Ni based catalyst (~1.3%) while the Pt based catalyst presented a drop of 1.4 wt.%, probably due to hydrogenation and/or hydrocracking reactions. The product distribution also shows that with the Ni based catalyst the gain in RON is mainly obtained from isomerization and probably aromatic alkylation reactions. In contrast, the gain in RON for the Pt based catalyst is mainly achieved through isomerization reactions.

Table 9
Product distribution obtained after hydroconversion of hydrotreated FCC gasoline[a]

| | Hydrotreated FCC gasoline (wt.%) | Metal($x$%)/HZSM5(10)–$Al_2O_3$ | |
|---|---|---|---|
| | | Ni(3.5) (wt.%) | Pt(0.3) (wt.%) |
| Paraffins | 10.82 | 9.9 | 10.3 |
| Isoparaffins | 29.94 | 32.1 | 32.8 |
| Olefins | 0.38 | 0.9 | 0.8 |
| Naphthenes | 14.81 | 11.5 | 14.3 |
| Aromatics | 34.5 | 35.8 | 33.1 |
| RON | 84.8 | 88.3 | 87.7 |
| Liquid yield (%) | 100.0 | 90.4 | 89.0 |
| Barrel-octane | 84.8 | 79.8 | 78.1 |

[a] Operating conditions: $T$ = 588 K, $P$ = 28 kg/cm$^2$, LHSV = 5.2 h$^{-1}$, $H_2$/HC = 850 ft$^3$/barrel.

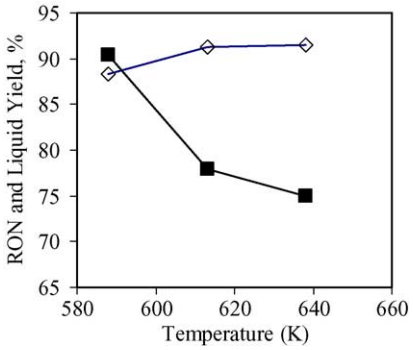


Fig. 2. Hydroconversion of hydrotreated FCC gasoline using a Ni(3.5%)/HZSM5(10)–alumina catalyst. Effect of temperature over RON (◇) and liquid yield (■).

Fig. 2 shows the effect of the temperature on the RON and liquid yield after hydroconversion of the FCC gasoline with the pre-sulfided Ni(3.5%)/HZSM5–alumina catalyst. These experiments were performed at 28 kg/cm$^2$ with a hydrogen to hydrocarbon ratio of 850 ft$^3$/barrel. This figure shows that by increasing the temperature from 588 to 638 K a gain in RON of 4 units and a drop in liquid yield of 15% is obtained. A similar although less drastic effect is observed by decreasing the LHSV from 7.3 to 1.3 h$^{-1}$ (Fig. 3).

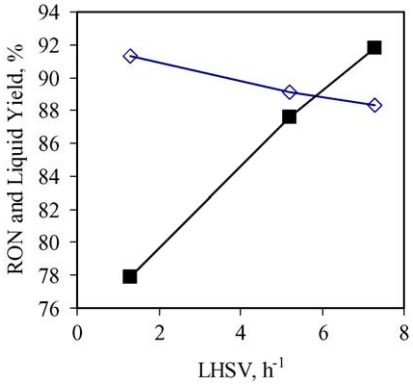


Fig. 3. Hydroconversion of hydrotreated FCC gasoline using Ni(3.5%)/HZSM5(10)–alumina. Effect of LHSV over RON (◇) and liquid yield (■).

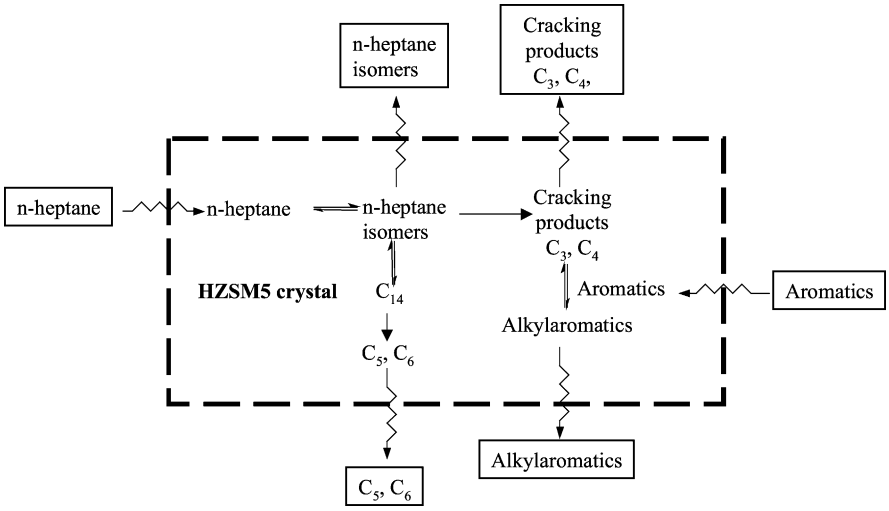


Fig. 4. Simplified reaction–diffusion scheme for the hydroconversion of *n*-heptane–benzene–toluene over monofunctional HZSM5(*x*)–$Al_2O_3$ catalysts.

It must be said that with the catalysts used here although there is an increase in RON for the FCC gasoline, there is also a loss of liquid yield, which leads to a decrease in barrel-octane. This decrease in barrel-octane is not observed with the model feed possibly because of the absence of isoparaffins, which are easily hydrocracked. Thus, to improve the catalyst performance emphasis should be placed in the tuning of the acid function in order to increasing the liquid yield while maintaining the isomerization and alkylation reaction routes. It should also be necessary to explore the operating conditions (temperature, pressure, and LHSV) at which the barrel-octane of the product is maximized.

### 3.2.4. Main reaction pathways

*3.2.4.1. Monofunctional catalysts.* Fig. 4 presents the main routes of reaction observed during the selective hydroconversion of the synthetic mixture over monofunctional HZSM5(*x*)–alumina catalysts. The individual steps in the reaction scheme have been well documented in the literature [19–21]. Since the reaction steps are performed exclusively over the acid sites, the initiation and termination steps are carried out through protolysis and hydrogen transfer reactions, respectively. A detailed hydroconversion study with the individual components (*n*-heptane, benzene, and toluene) and their mixtures, indicates that *n*-heptane transforms by a consecutive mechanism of isomerization–

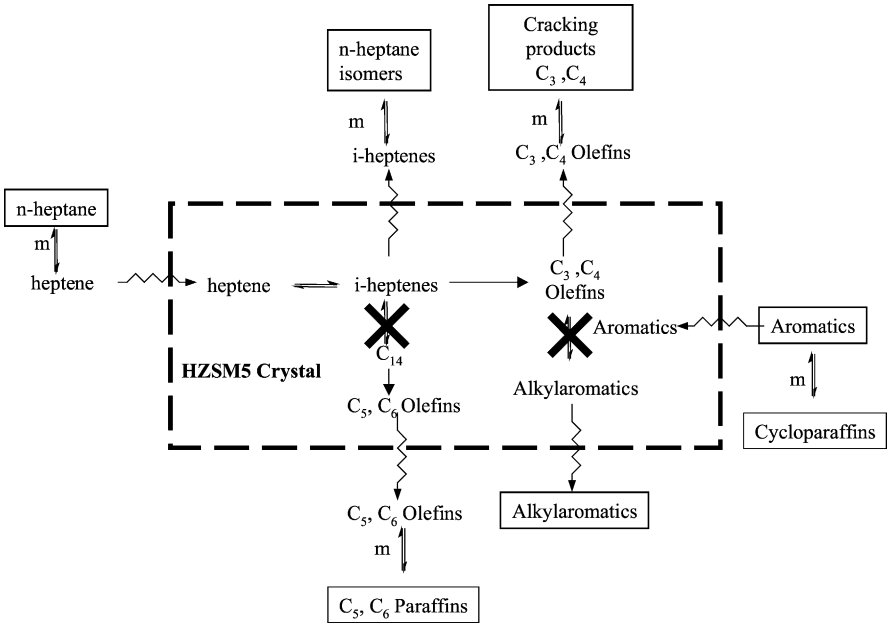


Fig. 5. Simplified reaction–diffusion scheme for the hydroconversion of *n*-heptane–benzene–toluene over pre-reduced Pt/HZSM5(10)–$Al_2O_3$ catalyst.

cracking in line with previous studies over similar catalysts [2,22]. It was also inferred that the dimerization–cracking route was important in this process, leading to significant amounts of $C_5$ and $C_6$ hydrocarbons, without a significant production of $C_1$ and $C_2$ compounds, as observed previously [3,23].

Toluene and benzene did not show any catalytic activity when reacted individually over the monofunctional catalyst. However, when they were transformed in the presence of *n*-heptane, a significant increase in aromatics conversion was observed, which results from the reaction of olefins produced during *n*-heptane cracking with the aromatics present in the mixture, giving $C_9$ and $C_{10}$ alkyl-aromatics as the main products.

The shape selectivity effects were also present during the hydroconversion of the model mixture. Therefore, in Fig. 4 the main reaction pathways are presented along with the diffusion steps through the zeolite cavities. These effects were evident from the low production of di-branched *n*-heptane isomers, which is restricted in the cavities of the HZSM5 zeolite. In addition, the 2-methylhexane/3-methylhexane ratio which took a value close to 2 at low *n*-heptane conversions, is in line with the results of Raybaud et al. [24] who found an increase in this ratio as the pore structure became more restricted.

*3.2.4.2. Bifunctional catalysts.* In the presence of a strong metallic function, as that of the pre-reduced Pt-based catalyst, the hydrogenation–dehydrogenation steps are carried out over the metallic sites, to produce olefins. For this catalyst the metallic species are located mainly over the alumina phase [25], so in Fig. 5 those species are represented outside the zeolite crystal. Although there is some separation between both zeolite and metallic catalytic phases, the intimacy criterion proposed by Weisz [26] is satisfied for this catalyst, indicating an adequate cooperation between the metallic and acid sites in this system.

Once carbenium ions are produced by protonation of the olefins over the acid sites, they can follow several routes [19–21]. One would be their isomerization, through a protonated cyclopropane intermediary, followed by hydrogenation over the metallic sites. Carbenium ions can also undergo cracking to produce smaller olefins and paraffins. Over this catalyst due to the strong metallic function, olefins hydrogenation reactions are favored, thus both aromatics alkylation and dimerization/cracking routes are almost suppressed, whereas the *n*-heptane isomerization route is notably favored, as reported previously for similar catalysts [2].

*3.2.5. Gain in RON, loss of liquid yield, and gain in barrel-octane*

Fig. 6 presents the behavior of different catalysts formulations in terms of the gain in RON, loss of liquid yield, and gain in barrel-octane for the model mixture. The former parameter (ΔRON) is defined as the difference between the RON of the product minus that of the feed. A similar definition is applied for the gain in barrel-octane

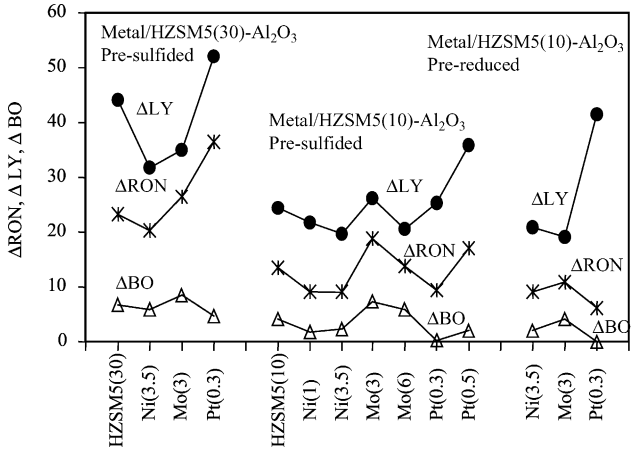


Fig. 6. Gain in RON (ΔRON), loss of liquid yield (ΔLY), and gain in barrel-octane (ΔBO) for different catalysts formulations.

(ΔBO), while the loss of liquid yield is the weight percent of liquid transformed to light hydrocarbons $C_4-$ (ΔLY). In order to improve the gain in barrel-octane it is required to increase the catalytic activity, diminishing at the same time the production of light hydrocarbons, and increasing simultaneously the production of isomers and alkyl-aromatics. A catalyst with these properties would allow us to work at lower temperatures, limiting the cracking reactions and improving the liquid yield as well as the gain in RON. Mo based catalysts appear to have these characteristics and therefore presented a higher gain in barrel-octane when compared with Ni or Pt based catalysts.

## 4. Conclusions

The results of this study clearly indicate that changes in the acid/metal balance, induced by the type of metal, metal loading, and initial state of the metal (reduced or sulfided) of Metal/HZSM5–alumina catalysts, can substantially modify the main routes of reaction and therefore, lead to important changes in the overall selectivity during the hydroconversion of a model mixture of hydrocarbons and hydrotreated FCC gasoline.

The drastic change in selectivity observed for the pre-reduced Ni and Pt based catalysts, is due to a substantial modification in the balance between the acid and hydrogenating functions of the catalyst. In the case of the Pt-based catalyst, the acid/hydrogenating functions balance is shifted in favor of the *n*-heptane isomerization route. At the same time, the hydrogenation of the olefinic intermediaries and the hydrocracking of *n*-heptane over the metallic sites of the catalyst are enhanced, leading to a low yield of alkyl-aromatics along with a high production of light hydrocarbons.

The generation of metal sulfides reduces the hydrogenating power of the metallic phase and, at the same time, increases the acid function because of the creation of new

acid sites, thus leading to a behavior closer to that of the acid monofunctional catalyst.

The Mo-based catalysts showed a well-balanced behavior between the gain in RON and loss of liquid yield of the model mixture, giving as a consequence the highest gain in barrel-octane.

The incorporation of a higher Mo loading (9 wt.%) cause a partial blockage of the zeolite pores imposing additional diffusional restrictions, and making difficult the alkylation reactions, therefore lowering the trapping efficiency of the catalyst.

## Acknowledgments

We acknowledge the financial support from PEMEX-Refinación, CONACyT and IMP-FIES programs.

## References

[1] A. Corma, V. Fornes, et al. in: B. Imelik (Ed.), Catalysis by Acids and Bases, Elsevier, Amsterdam, 1985, p. 409.
[2] G.E. Giannetto, G.R. Perot, M.R. Guisnet, Ind. Eng. Chem. Prod. Res. Dev. 25 (1986) 481.
[3] E. Blomsma, J.A. Martens, P.A. Jacobs, J. Catal. 155 (1995) 141.
[4] N.Y. Chen, W.E. Garwood, R.H. Heck, Ind. Eng. Chem. Res. 26 (1987) 706.
[5] A. Chica, A. Corma, J. Catal. 187 (1999) 167.
[6] L.D. Krenzke, J.E. Kennedy, K. Baron, M. Skripek, Paper Presented at the 1996 NPRA Annual Meeting, 17–19 March, San Antonio, Texas, 1996.
[7] A. Lugstein, A. Jentys, H. Vinek, J. Chem. Soc. Faraday Trans. 93 (1997) 1837.
[8] H. González, J. Ramírez, R. Zarate, T. Cortez, Ind. Eng. Chem. Res. 40 (2001) 1103.
[9] A. Gutierrez, H. González, J. Ramírez, G. Busca, Ind. Eng. Chem. Res. 16 (2001) 3423.
[10] K.M. Minachev, Y.I. Isakov, in: J. Rabo (Ed.), Zeolite Chemistry and Catalysis, ACS Monograph, 171, A.C.S., 1976.
[11] S. Bhatia, Zeolite Catalysis: Principles and Applications, CRC Press Inc., Boca Raton, FL, 1990.
[12] G. Clet, J.M. Goupil, G. Szabo, D. Cornet, J. Mol. Catal. A: Chem. 148 (1999) 253.
[13] H. González, R. Rodríguez, Ph.D. Thesis, Faculty of Chemistry, UNAM, México, 2003.
[14] M. Guisnet, P. Magnoux, et al. in: E.G. Derouane (Ed.), Zeolite Microporous Solids: Synthesis, Structure and Reactivity, NATO ASI Series, vol. 352, 1992, p. 437.
[15] T.F. Degnan, C.R. Kennedy, AIChE J. 39 (1993) 607.
[16] V. Keller, F. Barath, G. Maire, J. Catal. 189 (2000) 269.
[17] R. López Cordero, F.J. Gil Llambias, A. López Agudo, Appl. Catal. 74 (1991) 125.
[18] N.Y. Topsøe, H. Topsøe, J. Catal. 139 (1993) 641.
[19] P. Vogel, Carbocation chemistry, in: Studies in Organic Chemistry, Elsevier, Amsterdam, 1985.
[20] A. Olah, A. Molnar, Hydrocarbon Chemistry, J. Wiley and Sons. Inc., 1995.
[21] H. Pines, The Chemistry of Catalytic Hydrocarbon Conversions, Academic Press, New York, 1981.
[22] A. Patrigeon, E. Benazzi, C. Travers, J.Y. Bernhard, Catal. Today 65 (2001) 149.
[23] J. Meusinger, J. Liers, A. Mosch, W. Reschetilowski, J. Catal. 148 (1994) 30.
[24] P. Raybaud, A. Patrigeon, H. Toulhoat, J. Catal. 197 (2001) 98.
[25] J.F. Le Page, Applied Heterogeneous Catalysis, Design, Manufacture use of Solid Catalysts, Editions Technip, Paris, Francia, 1987.
[26] P.B. Weisz, Adv. Catal. 13 (1962) 137.